FULL PAPER DOI: 10.1002/adsc.201801591

Flavin-Dependent Halogenases from *Xanthomonas campestris* pv. campestris B100 Prefer Bromination over Chlorination

Mohamed Ismail,[a, c] Marcel Frese,[a] Thomas Patschkowski,[b] Vera Ortseifen,[b] Karsten Niehaus,[b] and Norbert Sewald[a,*]

[a] Organic and Bioorganic Chemistry, Department of Chemistry, Bielefeld University, Universitätstaße 25, 33615 Bielefeld (Germany)
Tel. int +49-(0)521-106 2051
Fax int +49-(0)521-106 156963
E-mail: norbert.sewald@uni-bielefeld.de

[b] Proteome and Metabolome Research, Department of Biology, Bielefeld University, Universitätstaße 25, 33615 Bielefeld (Germany)

[c] Department of Microbiology, Faculty of Science, Helwan University, Ain Helwan, Helwan, Cairo 11795, Egypt

Manuscript received: December 10, 2018; Revised manuscript received: February 9, 2019;
Version of record online: March 12, 2019

Supporting information for this article is available on the WWW under https://doi.org/10.1002/adsc.201801591

Abstract: Flavin-dependent halogenases selectively introduce halogen substituents into (hetero-)aromatic substrates and require only molecular oxygen and halide salts for this regioselective oxidative CH-functionalization. Genomic analysis of *Xanthomonas campestris* pv. campestris B100 identified three novel putative members of this enzyme class. They were shown to introduce halogen substituents into, e.g., substituted indoles, while preferring bromide over chloride.

Keywords: halogenases; bromination; regioselectivity; *Xanthomonas*

Introduction

Regioselective activation of carbon-hydrogen bonds is a valuable but also challenging approach to build up larger molecule structures and to incorporate functional groups in organic scaffolds for further derivatization. The regioselective incorporation of halogen substituents in aromatic and heteroaromatic compounds conveniently allows a plethora of follow-up transformations like metal-catalyzed cross-coupling reactions or nucleophilic substitutions. Halogenation by chemical synthesis requires molecular halogen and in the case of aromatic substrates, corrosive Lewis acid catalysts. Regioselectivity often is the key challenge and not always easy to achieve.[1,2]

Nature has evolved several strategies to generate halogenated natural products with interesting biological activities.[3] In many cases, both the type and the position of the halogen substituent in such metabolites exert a great influence on the biological activity.[4] Halogenated secondary metabolites with antibacterial, antifungal, or antitumor activity have been isolated from different organisms like bacteria, fungi, algae or plants,[5–8] which sparked investigations on their biosynthesis, in particular on the key step, the enzymatic halogenation.[9]

As chloride is the most abundant halide in the geosphere, chlorinated natural products prevail over other halogenated compounds. Enzymatic halogenation follows different chemical strategies and the halogenases can thus be classified according to their mechanisms of action. Fluorinases utilize fluoride for halogenation by nucleophilic substitution, but are limited to a few substrates.[10] α-Ketoglutarate-dependent halogenases introduce halide substituents (chloride, bromide) regioselectively even at non-activated aliphatic positions via a radical mechanism and usually require a substrate bound to a carrier protein.[11–13] Haloperoxidases and flavin-dependent halogenases generate hypohalous acid from halide salts for aromatic electrophilic substitution (S_EAr). While haloperoxidases use hydrogen peroxide for that purpose,[14] flavin-dependent halogenases convert molecular oxygen into a flavin hydroperoxide intermediate.[9]

Recently, enzymes have been getting more and more involved in chemical conversions due to their remarkable specificity and selectivity. The selective halogenation of non-activated CH bonds that only

relies on halide salts and oxygen under ambient conditions certainly is a 'dream reaction' of organic chemistry. However, not all available halogenases meet the requirements with respect to specificity and selectivity: Haloperoxidases release freely diffusible hypohalous acid and, hence, lack selectivity.[9,15]

Dairi et al. identified in 1995 the gene encoding an enzyme responsible for the chlorination of tetracycline that did not display any resemblance to haloperoxidases.[16] Few years later, a second member of this novel enzyme class was identified in *Pseudomonas fluorescens* BL915 and was named PrnA. It is a flavin-dependent halogenase that is involved in the biosynthesis of pyrrolnitrin.[17]

Flavin-dependent halogenases like PrnA catalyze halogenation of aromatic substrates with high specificity and regioselectivity, often regardless the presence of a directing group within the substrate.[18] Some of these enzymes are involved in polyketide synthesis or non-ribosomal peptide synthesis and require a carrier-bound substrate, while others accept soluble substrates.[19–21] Subsequent to the discovery of the tryptophan 7-halogenase PrnA, several other flavin-dependent halogenases have been characterized; e. g. KtzQ and KtzR from actinobacteria *Kutzneria Sp.* that are involved in the dichlorination at C6 and C7 position of tryptophan during the biosynthesis of the antifungal natural product kutzneride.[22] PyrH from *Streptomyces rugosporus* halogenates tryptophan at position 5 in pyrroindomycin biosynthesis.[23] RebH from *Lechevalieria aerocolonigenes* catalyzes regioselective halogenation of tryptophan at position 7 in the rebeccamycin biosynthesis.[24] Thal, another flavin-dependent halogenase involved in the biosynthesis of thienodolin in *Streptomyces albogriseolus,* was found to regioselectively chlorinate and brominate tryptophan at position 6.[25]

In all flavin-dependent halogenases conserved sequence signatures and structural features were distinguished. They are believed to play an important role in the identification and mechanism of action of this enzyme group. For instance, the presence of the motif GxGxxG within the flavin binding domain that is also conserved in all flavin-dependent enzymes plays an important role in binding of the flavin cofactor to the enzyme. Another motif, WxWxIP, located at the flavin binding domain, is believed to block binding of the substrate near the flavin cofactor, and hence to prevent halogenases from functioning as monooxygenases.[21,26]

The groups of van Pée and Walsh pioneered the discovery and characterization of flavin-dependent tryptophan halogenases and largely contributed to the elucidation of the enzyme mechanism.[27,28] The reaction proceeds through the oxidation of the reduced flavin cofactor ($FADH_2$) with molecular oxygen generating a C4α-hydroperoxyflavin (FAD-OOH). This reactive intermediate is attacked by the halide nucleophile to form hypohalous acid (HOX). The crystal structure[29,30] reveals that HOX has to diffuse through a 10 Å long tunnel that separates the flavin binding site from the active site pocket. The proposal of HOX reacting with a conserved active site lysine residue generating an *N*-haloamine as halogenating agent is still under debate.[27] The Wheland complex formed upon attack of the halonium electrophile on the aromatic substrate is subsequently deprotonated by a conserved glutamate residue generating the halogenated product (Scheme 1).[30–34]

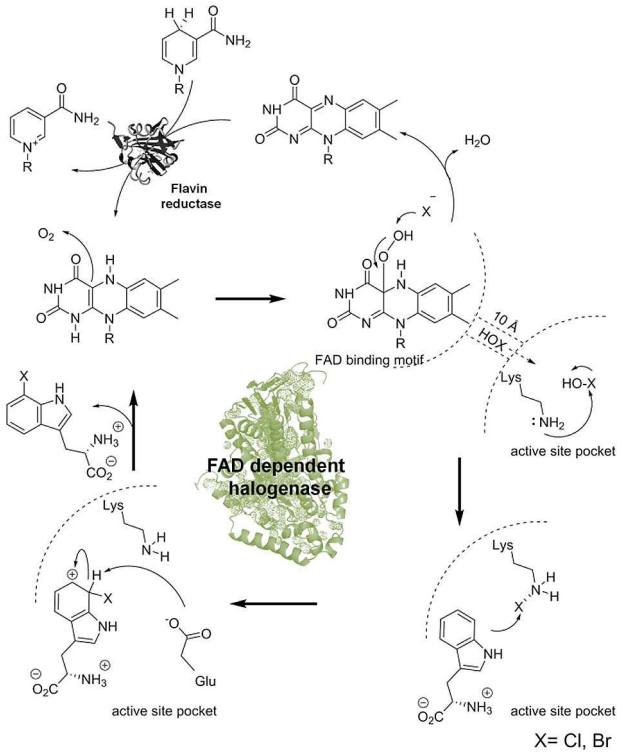

Scheme 1. Schematic view of the catalytic mechanism of flavin-dependent tryptophan halogenases (e. g. RebH) combined with the enzymatic cofactor regeneration system using flavin reductase.

In general, flavin-dependent halogenases exhibit low to moderate activity.[35] A recent theoretical study attempting to identify the possible mechanism of the halogenation reaction revealed that one of the rate limiting steps is the deprotonation of the Wheland intermediate by a glutamate residue.[36] The flavin binding domain on the other hand also influences the rate of hypohalous acid generation and its transfer to the active site and, hence, the overall rate of halogenation reaction.

The regioselectivity of the enzymatic halogenation is mainly based on steric and entropic factors. The amino acid residues located at the active site entrance

and pocket control substrate access and orientation. Hence, the position of halogenation mainly is independent from the presence of directing groups within the aromatic ring.[26,33] Because of these key advantages, FAD-dependent halogenases recently attracted more and more attention as valuable biocatalysts for chemical transformations. Investigations on novel halogenases or engineering the existing ones, for broader substrate scope, enhanced activity, and stability have been conducted.[18,37–41]

Xanthomonas comprises a group of Gram negative *Proteobacteria* infecting over 350 monocotyledonous and dicotyledonous plant species.[42] The plant pathogen *Xanthomonas campestris* (*Xcc*) is a member of this group infecting crucifers like cabbage and cauliflower. It causes black rot disease by invading the vascular tissue of the host plant.[42] They produce a characteristic yellow pigment called xanthomonadin, a mixture of brominated aryl polyene esters considered as a chemotaxonomic feature for *Xanthomonas sp.*[43] In addition, they secret the exopolysaccharide xanthan, commercially known as xanthan gum. It is employed, e.g., as thickening agent and emulsifier in food and pharmaceutical industry. Consequently, xanthomonads are considered an important group of bacteria for their commercial, biotechnological application and their economic importance as plant pathogen.[44,45] Besides, they might be a source for novel halogenases, considering the brominated xanthomonadin, with new substrate spectrum.

Results and Discussion

In the frame of our studies directed towards the discovery of novel halogenases, we investigated three novel putative flavin-dependent tryptophan halogenases, identified and cloned from the genome of the xanthan producing *Xanthomonas campestris* pv. campestris B100 strain.[46]

Identification of *Xcc* Halogenases

The whole genome of *Xanthomonas campestris* pv. campestris strain B100[46] (Accession no.: PRJNA436896) was screened for the signature motifs GxGxxG and WxWxIP present in the FAD binding domain and that are consensus and characteristic for the whole flavin-dependent tryptophan halogenases. Three genes were identified and annotated as tryptophan halogenases, namely xcc-b100_1333, xcc-b100_4156, and xcc-b100_4345. However, further structural and functional characterization was necessary to confirm their class and activity.

Expression of *Xcc* Halogenases

In order to verify the results of the gene annotation, the three putative halogenases were produced recombinantly in *E. coli* as previously reported for other cases with co-expression of the chaperons groES and groEL. Under these conditions, all halogenases were obtained in soluble form.[47,48] SDS-PAGE analysis of the purified proteins indicated a molecular mass of ~60 kDa for *Xcc*4156, while *Xcc*1333 and *Xcc*4345 have lower molecular masses of ~55 kDa matching the calculated values of 58 kDa for *Xcc*4156 and 56 kDa for both *Xcc*1333 and 4345 (Figure S1). The *Xcc* halogenases were further analyzed biochemically using the monochlorodimedon assay[29] to exclude haloperoxidase activity. In this assay, the activity of the halogenase can be monitored photometrically due to the halogenation of an artificial substrate, monochlorodimedon, which readily reacts in solution with HOX to give its geminal dihalogenated derivative.[49] In a reaction mixture containing monochlorodimedon, the flavin cofactor, flavin reductase PrnF and alcohol dehydrogenase (enzymatic regeneration system) were excluded (Scheme 1). No halogenation of monochlorodimedon could be detected in presence and absence of the *Xcc* halogenases.

Although their natural substrates are still unknown, the *Xcc* halogenases share a high pairwise identity to tryptophan halogenases like RebH, PrnA and PyrH (Figure S2). Therefore, tryptophan and indole derivatives were selected for a preliminary substrate screening. In addition, different halide salts (NaCl, NaBr, NaI) were investigated for the halogenation of the accepted substrates. Initial screening revealed that bromination of indole and some indole derivatives was possible, but not chlorination. Tryptophan surprisingly was not accepted by all three halogenases, despite their annotation as tryptophan halogenases. Hence, indole was used as a substrate for further optimization. A buffer screening showed that 50 mM Na_2HPO_4 at pH 7.4 led to the highest halogenase activity (Figure S3).

The storage stability of the purified enzymes at 4 °C was also investigated using indole as substrate. Activity was retained for more than three weeks, leading to 100% conversion of 1 mM indole using 21 mol% (12.4 mg mL^{-1}) of *Xcc* halogenases.

Substrate Screening

Based on the initial results, a larger array of compounds was selected for a more elaborate substrate screening (Scheme S1). Enzymatic conversion was monitored by RP-HPLC, RP-HPLC-MS, and GC-MS to identify halogenated products. Besides using chloride as halide source, a particular interest was placed on bromide. Notably, the *Xcc* halogenases

Table 1. Total turnover number and regioselectivity of the three flavin-dependent halogenases with the brominated substrates.

Substrate	*Xcc*-B1004156[a]		*Xcc*-B1004345[b]		*Xcc*-B1001333[c]		M/I[c]
	TTN[b]	Position[a]	*TTN*[b]	Position[a]	*TTN*[b]	Position[a]	
Indole	11.9 ± 4	3	33.3 ± 9	–	58.4 ± 3	3	NR
5-Hydroxytryptophan	< 1	6	12.6 ± 3	6	> 1	–	+M/−I
Tryptophol	1.7 ± 2	7	9.8 ± 1	7	8.1 ± 1	7	+I
7-Azaindole	< 1	–	5.4 ± 1	3	21.8 ± 5	3	NR
Indole-5-carbaldehyde	< 1	–	> 1	–	> 1	3	−M/−I
5-Hydroxyindole	30.3 ± 8	2, 3	NA	NA	NA	NA	+M/−I
5-Cyanoindole	< 1	–	12.6 ± 1	3	10.2 ± 0.7	3	−M/−I
3-Formylindole	5.5 ± 0.6	–	NA	NA	NA	NA	−M/−I
3-(3-Indolyl)propionic acid	< 1	–	6.9 ± 13	7	> 1	7	+I
Phenol	4.9 ± 0.2	4	NA	NA	NA	NA	+M/−I
(3-Indolyl)acetonitrile	NA	NA	9.5 ± 0.7	–	NA	NA	+I
5-Methylindole	NA	NA	19.9 ± 2	2, 3	49.8 ± 1	2, 3	+I

[a] Regioselectivity of the *Xcc* halogenases.
[b] total turnover number.
[c] mesomeric and inductive effect of the different substrates, NA: not accepted, NR: not relevant.

investigated were found to exclusively brominate the substrates indole, 7-azaindole, 5-hydroxytryptophan, tryptophol and other heterocyclic derivatives, even in the presence of an excess of chloride (Table 1). Although the three enzymes share little identity on the sequence level (49–50%), they showed nearly similar substrate scope.

Regioselectivity of Enzymatic Halogenation

The reactions were scaled up and performed on a semi-preparative scale to determine the regioselectivity of the enzymatic halogenation. Each *Xcc* halogenase was precipitated with ammonium sulfate together with the auxiliary enzymes PrnF and ADH and immobilized with glutaraldehyde to yield cross linked enzyme aggregates (CLEA).[50,51] This approach was successfully applied in previous studies for the upscaling of enzymatic halogenation using the tryptophan 7-halogeanse RebH.[52]

The optimal glutaraldehyde concentration for the different halogenases was determined, as excessive cross-linking may lead to loss of enzymatic activity. 1% (v/v) glutaraldehyde was found to yield the highest conversion among the other tested glutaraldehyde percentages (Figure S4). Furthermore, the resulting CLEAs could be re-used in three batches while retaining halogenase activity (Figure S4).[53]

Several substrates could be halogenated using halogenase-CLEAs in sufficient amounts for structural elucidation by NMR spectroscopy, whereas other substrates were hardly converted (Table 1). Among all substrates tested so far, indole led to the highest conversions. MS analysis confirmed product formation, also showing the typical isotope pattern commonly observed for monobrominated compounds (Scheme 2). This is also true for the rest of the brominated substrates. NMR analysis revealed C^3 as bromination site, which is the electronically most favoured position for electrophilic substitution in the indole ring.[47] Notably, previous studies on the substrate scope of the tryptophan 7-halogenase RebH also showed chlorination of indole at the C^3 position of the pyrrole ring.[54]

In the halogenase, $FADH_2$ efficiently reacts with molecular oxygen to form a flavin-hydroperoxide. This reactive intermediate leads to hypohalous acid formation which subsequently halogenates the substrate. However, hydrolysis of the flavin-hydroperoxide results in the release of H_2O_2. This uncoupling side reaction is commonly observed in flavin-dependent enzymes like monooxygenases and halogenases ("oxygen dilemma").[55–57] It leads to a loss of reducing equivalents required for product formation, while forming H_2O_2 as a strong oxidant. Reactive oxygen species (ROS) have been shown to affect e.g. the stability of dehydrogenases by oxidation of cysteine and methionine residues.[58–60] The oxygen dilemma can be levied by addition of superoxide dismutase or catalase to the reaction. Therefore, it was important to add catalase to the preparative scale halogenation reactions for H_2O_2 elimination.

Indole bromination by the *Xcc* halogenases was found to proceed efficiently only after portionwise (e.g. daily) addition of catalase (Figure 1) to decompose hydrogen peroxide.[61] Without daily addition of catalase, the reaction was observed to stop, most likely due to halogenase and dehydrogenase inhibition. Attempts to co-immobilize catalase together with *Xcc* halogenase, flavin reductase and alcohol dehydrogenase revealed the instability of the immobilized catalase over time. After 4–5 days, the reaction rate declines

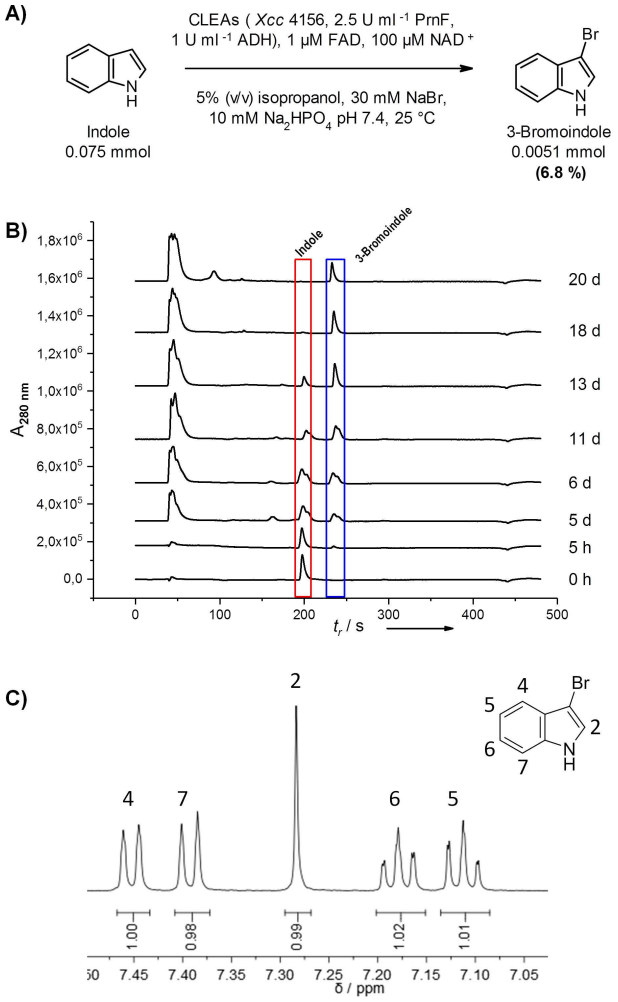

Scheme 2. (A) Scheme for the enzymatic bromination of indole using immobilized *Xcc*4156 halogenase (B) Enzymatic halogenation of indole to 3-bromoindole monitored over 21 days; (C) aromatic region of the ^{1}H-NMR spectrum of indole confirming bromination at C3 of the pyrrole ring, Reaction conditions: total volume 150 mL, 0.5 mM indole, 30 mM NaBr, 10 mM Na_2HPO_4 pH 7.4, 1 µM FAD, 0.1 mM NAD^+, 5% (*v/v*) isopropanol, daily addition of 1000 U catalase, co-immobilized *Xcc*4156 (from 1.5 L *E. coli* culture) 2.5 U mL^{-1} PrnF, 1 U mL^{-1} ADH, 150 rpm, 25 °C.

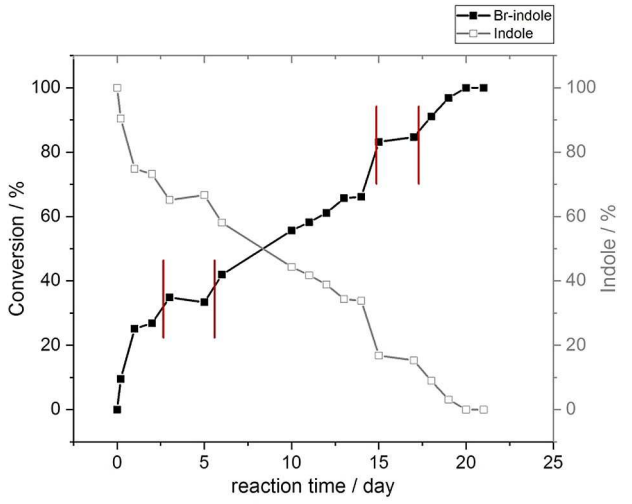

Figure 1. Time course of indole bromination by *Xcc*4156. Daily addition of 1000 U catalase was necessary for the reaction to proceed to full conversion within 21 days. The reaction slowed down significantly once catalase was omitted (lag periods marked in red). Most likely, non-enzymatic $FADH_2$ oxidation leads to H_2O_2 accumulation and lower reaction rates. Reaction conditions: total volume 150 mL, 0.5 mM indole, 30 mM NaBr, 10 mM Na_2HPO_4 pH 7.4, 1 µM FAD, 0.1 mM NAD^+, 5% (*v/v*) isopropanol, co-immobilized *Xcc*4156 (from 1.5 L *E. coli* culture) 2.5 U mL^{-1} PrnF, 1 U mL^{-1} ADH, 150 rpm, 25 °C.

and stops completely if no additional catalase is added to the reaction. This observation provides additional evidence that the *Xcc* halogenases do not belong to the class of haloperoxidases that utilize H_2O_2 to generate hypohalous acid in solution for non-regioselective halogenation. A control experiment using immobilized flavin reductase and alcohol dehydrogenase with the daily addition of catalase, but omitting the halogenase, confirmed that bromination is halogenase dependent.

The regioselectivity of the novel enzymes was investigated by selecting a panel of substrates based on different substituent patterns and electronic characteristics. While indole is being accepted by all enzymes leading to the formation of 3-bromoindole, C^3-substituted indoles (tryptophol, 3-formylindole, 3-(3-indolyl)propionic acid, (3-indolyl)acetonitrile) were converted only sluggishly. As the conversion of these 3-substituted substrates is low, only some products could be isolated in sufficient yields for structure elucidation. These compounds were shown to be brominated at the electronically unfavoured C^7 position (Scheme 3, Figure S5).[48,54] Despite the higher reactivity of the C^2 position of the pyrrole ring, the regioselectivity of the enzyme plays a role in directing the halogenation to the less reactive C^7 position instead. Indole derivatives with substituents at the benzene ring like 5-hydroxyindole are only accepted by *Xcc*4156. 5-methylindole is accepted by each of *Xcc*4345 and 1333 with low to moderate activity, whereas 5-cyanoindole is sluggishly brominated by all three halogenases. Noteworthy, 7-azaindole and also 3-formylindole could be halogenated to a small extent with *Xcc*4156 (Table 1), however providing insufficient amounts for NMR analysis. 5-Hydroxytryptophan, whose C^3 position is substituted with the amino acid backbone, was brominated in the C^6 position. This is in agreement with the *ortho*-directing effect exerted by the hydroxyl functionality (Figure S6).[48]

Docking and molecular dynamics simulation studies with tryptophan and 5-hydroxytryptophan on the *Xcc*4156 confirmed that both substrates can access the

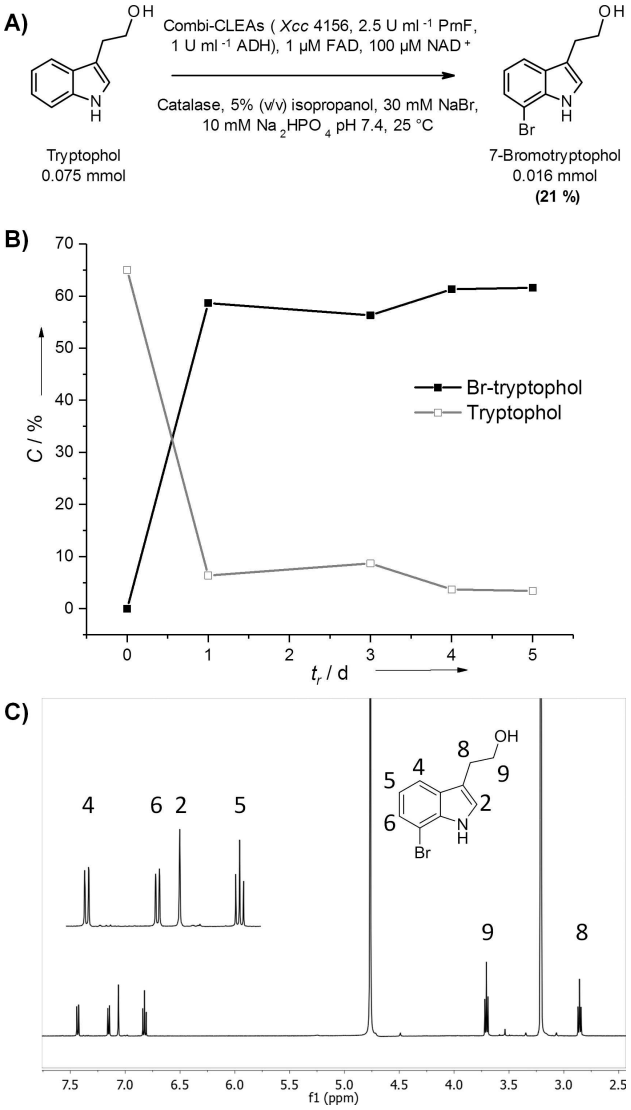

Scheme 3. (A) Semi-preparative bromination of tryptophol using *Xcc*4156 combi-CLEAs; (B) 60% conversion was achieved after 6 d, followed by purification using preparative HPLC. (C) The brominated product was analyzed with ^{1}H NMR spectroscopy and structure elucidation revealed C^7 as the bromination site. LC-MS and HRMS confirmed the mass of the product. Reaction conditions: total volume 150 mL, 0.5 mM tryptophol, 30 mM NaBr, 10 mM Na_2HPO_4 pH 7.4, 1 µM FAD, 0.1 mM NAD^+, 5% (*v/v*) isopropanol, co-immobilized *Xcc*4156 (from 1.5 L *E. coli* culture) 2.5 U mL^{-1} PrnF, 1 U mL^{-1} ADH, 150 rpm, 25 °C.

active site. In contrast to 5-hydroxytryptophan, tryptophan binding was not stabilized by hydrogen bonding or other interactions within the active site throughout the simulation time (1 ns, data not shown). This explains the inability of the *Xcc* halogenases to brominate tryptophan. The hydroxyl group of 5-hydroxytryptophan is involved in the formation of a hydrogen bond with Glu337. This is also true for other tryptophan halogenases (RebH and PyrH) where tryptophan is stabilized by hydrogen bonding, maintaining its correct positioning within the active site for the halogenation to occur.[30]

On the other hand, dibromination products of 5-methylindole and 5-hydroxyindole could also be explained in the same sense. The stability of these substrates within the active site is more enhanced by their small size, facilitating the accessibility to the active site pocket. In addition, the presence of substituents like a hydroxyl group enables the interaction (by H-bonding formation) with amino acid residues within the active site. At the same time, these substituents also increase the electron density of the substrate to promote S_EAr. Nevertheless, a crystal structure of the novel halogenases soaked with these substrates would help understanding the selectivity issues.

Halogenation via S_EAr usually follows mesomeric and/or inductive effects of the substituents that influence the electron density in the aromatic ring and hence the site of halogenation. When the most nucleophilic C^3 position of the indole ring is occupied, bromination takes place in the six-membered ring and in case of 5-hydroxytryptophan the hydroxyl group directs bromination to the C^6 position due to its positive mesomeric effect. Similarly, phenol is brominated in the electronically favored *para* position. However, if the C^3 position of indole is unsubstituted, bromination takes place there, regardless of the substituents present on the benzene ring. This was observed with indole-5-carbaldehyde brominated with *Xcc*1333, as well as 5-cyanoindole brominated with both *Xcc*1333 and 4345. By blocking the electronically favored position 3 in the pyrrole ring for the electrophilic aromatic substitution and the absence of directing substituents on the benzene ring halogenation takes place at the C^7 position. This was observed with all three halogenases in the case of tryptophol and 3-(3-indolyl)propionic acid with *Xcc*4345 and 1333 (Table 1).

Total Turnover Number (*TTN*)

The total turnover number of the novel halogenases was determined to obtain information on the efficiency of the enzymes towards different substrates (Table 1). All enzymes display a relatively moderate to low *TTN* towards the tested substrates with values between 0 and 60. Remarkably, 5-hydroxytryptophan is converted by *Xcc*4345 with a *TTN* of 12, whereas tryptophan is not accepted by any investigated halogenase. In general, the *TTN* is higher for indole, 5-methylindole and 5-hydroxyindole, which indicates that indole, indole derivatives or smaller heterocyclic compounds accommodate better within the active site. Bulky

substituents are less tolerated according to the observed *TTN* (Figure S7).

Thermostability of *Xcc* Halogenases

Temperature is an important factor affecting the enzymatic activity and increased thermal stability of enzymes may be associated with improved turnover. *Xcc*4156 was found to be temperature sensitive and even at 30 °C the activity was largely reduced. *Xcc*1333 showed higher stability; with 23, 35, and 18% conversion of indole as substrate at 25, 30, and 37 °C after 7 hours of reaction time, respectively. *Xcc*4345 showed lower activity at 30 °C and the activity was dramatically reduced at 37 °C (Figure 2, S8). All *Xcc* halogenases were not active at 45 °C and precipitated. The stability profile of the three halogenases aligns with the observed *TTN,* where *Xcc*1333 showed the highest *TTN* against most of the tested substrates (Table 1).

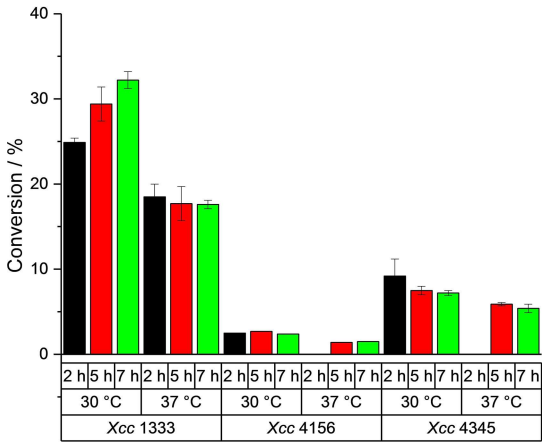

Figure 2. Time course of indole halogenation by the three *Xcc* halogenases at 30 °C and 37 °C as monitored by RP-HPLC. Reaction conditions: in 600 μL, 0.5 mM indole, 0.1 mM FAD, 20 mM nicotinamide mimic 1-benzyl-1,4-dihydronicotinamide,[35] 30 mM NaBr, 10 mM Na_2HPO_4 pH 7.4, 25 °C.

The protein stability was also investigated using circular dichroism spectroscopy and melting temperatures (T_m) of 46 °C and 47 °C were determined for *Xcc*4345 and *Xcc*4156, respectively, while *Xcc*1333 has a slightly higher T_m of 54 °C, which corresponds to the observed conversions at elevated temperature.

Homology Model and Structural Analysis of *Xcc* Halogenases

A homology model was established to provide information on the 3D structure and to enable alignment studies with other related enzyme structures. Blast analysis of *Xcc*4156, 1333 and 4345 sequences revealed the most related structures to the target sequence. The highest identity sequences for *Xcc*4156 were RebH with 33.6% and PrnA with 32.3% identity. *Xcc*1333 showed 33.1% identity to PyrH and 31% to RebH. *Xcc*4345 showed 36.0%, 35.8% and 32.9% identity to PyrH, PrnA, and RebH, respectively. Though the sequence identity was relatively low, it was confirmed that the *Xcc* enzymes have an FAD binding site and the active site residues conserved for flavin-dependent halogenases.

Hybrid homology models of *Xcc*4156 and 1333 were based on combined parts from 25 models built by YASARA Structure. Analysis of the built model was performed after aligning with apo-RebH, PyrH and PrnA, soaked with the substrate tryptophan and the flavin cofactor. It was assumed that the structures of *Xcc*4156 and *Xcc*1333 combine features of both RebH and PrnA.[30] One prominent difference compared to RebH concerns the loop (residues 40–48) covering bound FAD. In case of RebH, this loop is oriented away from the FAD, leaving it exposed to the surrounding environment. However, in case of *Xcc*1333 the loop (residues 41–19) covers FAD in a similar fashion as in PrnA. This is also true for *Xcc*4156 with slight structural deviation at the alloxazine moiety of FAD binding site. As a result of insertion and deletion, the α-helix covering the active site entrance in tryptophan halogenases is shorter in the *Xcc* halogenases, where a loop exists leaving the active site pocket exposed. *Xcc*1333 however, has a longer loop compared to *Xcc*4156, which might rigidify upon substrate binding covering the active site (Figure 3).

Obviously, the presence of such loops within the enzyme structure and in particular at the active site entrance may influence substrate specificity and kinetic characteristics of the enzyme. This was observed for RebH (PDB entry: 2OA1), where the α-helix covering the active site directly interacts with the substrate tryptophan forming hydrogen bonds with residues Tyr454, Glu461, Tyr455 and Phe465. The absence of such interactions in *Xcc* halogenases explains their inability to catalyze tryptophan halogenation.

Besides that, bulky residues are found within the active site of *Xcc*4156 and *Xcc*1333 that differ from tryptophan halogenases RebH. For instance, Ser434 in *Xcc*1333 is substituted by the polar residue Asn, while Phe430 in *Xcc*1333 is substituted by Trp and Val379 by Thr. In addition to the structural and residual differences within the active site, similar residues in both enzymes are found in different orientation towards or away from the active site cavity. Those changes would affect the interaction, orientation and stabilization of the substrates and hence affect substrate specificity and regioselectivity (Table S1).

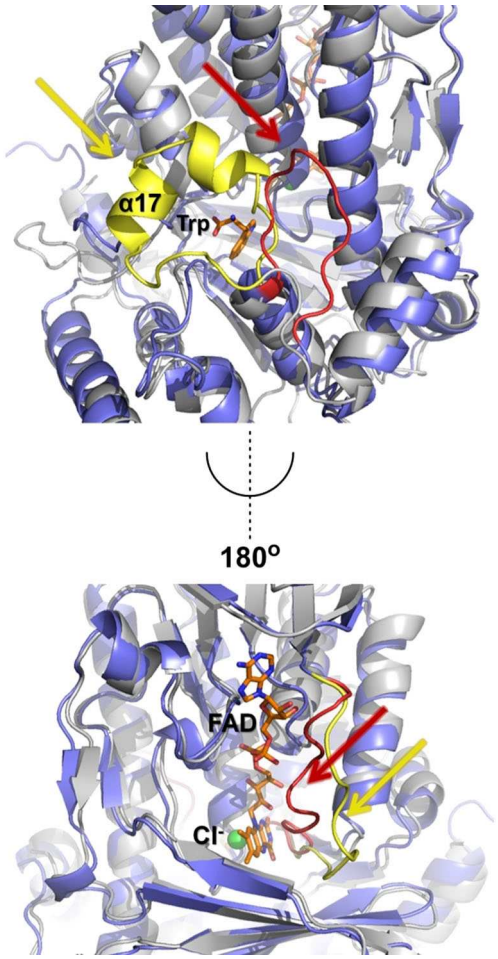

Figure 3. Superimposed homology model of *Xcc*1333 (blue) and crystal structure of RebH (grey, PDB entry: 2OA1) showing the active entrance secondary structure differences with an α-17 (yellow) covering the active site entrance in RebH, substituted by a short loop (red) in *Xcc*1333. On the other side of the protein is the FAD binding motif with flavin (orange) and chloride (green), showing the structural difference at the loop covering FAD in case of RebH (yellow) and *Xcc*1333 (red).

Further sequence analysis for *Xcc*4156 was performed in comparison with the sequences of other tryptophan halogenases; PyrH (GenBank: AAU95674.1), PrnA (GeneBank: AAB97504), Thal (GeneBank: ABK79936.1) and RebH (GeneBank: Q8KHZ8) (Figure S2). Notably, the signature motifs for FAD-dependent halogenases GxGxxG and WxWxIP, both highly conserved in all tryptophan halogenases, are present in the three *Xcc* halogenases as well.[26,29] In addition, the conserved residues that are believed to be directly involved in the halogenation within the active site, a distinct Lys and Glu residue, are also present in the three *Xcc* halogenases.[33]

The homology models built for *Xcc*4156 and *Xcc*1333 provided detailed insight into the active site pocket geometry. The three novel enzymes have 40–50% pairwise sequence identity within the active site and its surrounding. Nevertheless, a profound insight within the active site pocket and the residues that might be involved in the substrate binding, have revealed very high identity (>90%) with similar residues explaining the similar substrate specificity and regioselectivity of *Xcc* halogenases (Table S1).

Conclusion

Three putative flavin-dependent halogenase genes from different locations of the *Xanthomonas campestris* genome show high similarity to flavin-dependent halogenase genes with respect to the flavin binding site and active site residues. Despite having been annotated as tryptophan halogenases, the enzymes do not accept tryptophan as a substrate. The lack of the required interactions to stabilize tryptophan within the active site pocket might give an explanation. On the contrary, 5-hydroxytryptophan is being brominated as a result of a hydrogen bond formed between its hydroxyl group and Glu337. Indole and substituted indoles are being accepted. However, for bulkier substrates lower *TTN* was detected. Biochemical characterization revealed the ability of the halogenases to exclusively brominate their substrates, even in the presence of excess chloride salt. A difference in the amino acid residues surrounding the halide binding site could explain the bromide preference. However, the 10 Å tunnel connecting the FAD binding domain and the active site pocket could have an influence on the accessibility of the hypohalous acid for a selective transport towards the active site. Further structural characterization via site directed mutagenesis might help revealing the reason for bromide selectivity and also alter the substrate selectivity and enzymatic activity. Despite the low reaction rates exhibited by halogenases, they still accomplish regioselective halogenation reactions difficult to be effected by other conventional chemical approaches. The structural and biochemical investigation of the novel halogenases have expanded our knowledge on the flavin-dependent halogenases and will assist exploiting the enzymatic halogenation reactions.

Experimental Section

Sequence Analysis

The protein sequence of the target halogenases were blasted using UniProt blast with proteins of known 3D structure as target database and E-threshold of 10. The result was further used for sequence alignment using EMBL-EBI Clustal Omega multiple sequence alignment tool for generating the Neighbour Joining (NJ) phylogenetic analysis and for determining the sequence identity percentage.

Homology Models

The homology model for *Xcc*4156 was built using SWISS-MODEL server automated mode which relies on ProMod3 as modelling engine. More refined models of *Xcc*4156 and *Xcc*1333 were built with Yasara Structure using the default settings.[62] Further comparative analysis was conducted based on the alignment results of Clustal Omega.

Heterologous Gene Expression

For the heterologous expression of the Xcc-B100 halogenase genes *Escherichia coli* BL21(DE3) (Novagene) was transformed with the pET28a+ plasmid encoding the corresponding Xcc-B100 halogenase gene, as well as the pGro7 plasmid (Takara) for chaperone co-expression. 60 μg mL^{-1} Kanamycin and 50 μg mL^{-1} chloramphenicol were added to 1 L Luria-Bertani (LB) media, which was then inoculated with 20 mL of the preculture and incubated at 37 °C until it reached an OD_{600nm} of 0.6. Protein production was induced using 100 μM isopropyl-β-D-thiogalactopyranoside (IPTG) and 2 mg mL^{-1} L-arabinose. The temperature was lowered to 25 °C for the rest of the cultivation. The cells were harvested after 20 h by centrifugation (4000 × g, 30 min, 4 °C) and stored at −20 °C. For the production of the flavin reductase PrnF, *Pseudomonas fluorescens* strain BL915 ΔORF1-4 containing the expression vector pCIBhis-prnF was grown overnight at 30 °C in LB medium containing 30 μg mL^{-1} tetracycline. At 30 °C 1 L of LB medium with the appropriate antibiotics was inoculated with 10 mL of the overnight culture and cultivated for 3 d. The cells were harvested by centrifugation and stored at −20 °C. Production of the alcohol dehydrogenase from *Rhodococcus ruber* was conducted in *E.coli* BL21(DE3) previously transformed with pGro7 (Takara) and pET21-ADH. The preculture supplemented with 50 μg mL^{-1} chloramphenicol and 100 μg mL^{-1} ampicillin was grown overnight at 30 °C in LB medium. 20 mL of the preculture were used to inoculate 1 L LB medium containing the same antibiotics. The culture was grown at 30 °C until an OD_{600nm} of 0.3 was reached. At that point, the incubation temperature was lowered to 25 °C, 0.5 mM $ZnCl_2$ and 2 mg mL^{-1} L-arabinose were added. Induction of ADH expression was done using 0.1 mM IPTG at OD_{600nm} of 0.6. The cells were harvested after 16 h by centrifugation and kept at −20 °C.

Enzyme Purification

For purification of His_6-tagged *Xcc* halogenase and flavin-reductase PrnF, 1.5 L of *E. coli* culture was resuspended by vortexing in 30 mL 100 mM NaH_2PO_4 buffer (pH 7.4) and lysed three times by French Press (1000 psig). The total lysate was centrifuged (10000 × g, 45 min, 4 °C) and filtered through a 0.45 μM Whatman filter. The soluble fraction was injected (flowrate 0.5 mL min^{-1}) on a pre-equilibrated HisTALON agarose affinity column with 50 mM NaH_2PO_4, pH 7.4, 300 mM NaCl or NaBr (equilibration buffer). The column was washed with 15 mL equilibration buffer (flow 1 mL min^{-1}) followed by 20 mL 50 mM NaH_2PO_4, 10 mM imidazole, pH 7.4, 300 mM NaCl or NaBr (washing buffer, flow 1 mL min^{-1}). The protein was eluted in 0.5 mL aliquots with 50 mM NaH_2PO_4, 300 mM imidazole, pH 7.4, 300 mM NaCl or NaBr (elution buffer, flow 0.5 mL min^{-1}). 10% sodium dodecyl sulfate polyacrylamide gel electrophoresis (SDS-PAGE) was used for the analysis of different fractions during the course of protein purification. Alcohol dehydrogenase ADH was purified via heat precipitation by heating the lysate from 1.5 L of culture to 60 °C for 20 min, followed by centrifugation to remove denatured proteins. The supernatant was stored at −20 °C.

Chemical Analysis and Product Purification

Reactions were monitored by using RP-HPLC on a Thermo Scientific Accela 600 equipped with a Thermo Scientific Hypersil GOLD 3 mm column (C18, 150 × 2.1 mm, solvent A $H_2O/CH_3CN/TFA = 95:5:0.1$, solvent B $H_2O/CH_3CN/TFA = 5:95:0.1$, with a flow of 0.7 mL min^{-1} using a gradient from 0–100% B over 5 min). LC/MS analysis was accomplished by using a AllianceHT 2795 HPLC system equipped with C8 Symmetry column (length: 100 mm, diameter: 2.1 mm, particle size: 3.5 μm), coupled with a Waters micromass ZQ2000 ESI-MS (gradient in 10 min from 5% B to 95% B, back to 5% B in 0.2 min, total run time 25 min at a flow of 400 μL min^{-1}, solvent A H_2O:HCOOH 100:0.1, solvent B of CH_3CN:HCOOH 100:0.1). GC-MS analysis was done using TRACE GC coupled to a Polaris Q mass spectrometer (Thermo Fisher Scientific), equipped with VF-5 MS column (30 m × 0.25 mm, 5% diphenylsiloxane, 95% dimethylsiloxane 0.25 μm). The temperature gradient program was 3 min, 80 °C, a ramp with 5 °C min^{-1} up to 325 °C and finally 325 °C for 2 min. The MS transfer line temperature to the quadruple was set to 250 °C and the electron impact (EI) ion source temperature was 220 °C. The spectra were recorded with a scanning range of 50–750 mz^{-1}. High resolution mass spectrometry (HRMS) was done using an Agilent 6220 accurate-mass TOF LC/MS with Hypersil Gold C18 (50 mm × 2.1 mm, 1.9 μm particle size), eluent A: H_2O:CH_3CN:HCOOH = 95:5:0.1 and eluent B: H_2O:CH_3CN:HCOOH = 5:95:0.1 with a gradient from 0 to 98% B over 9 minutes. Purification of the compounds was performed by preparative HPLC on a LaChrom System (Merck Hitachi) equipped with a Phenomenex Jupiter column (10 mm, C18, 300 Å, 250 × 21.1 mm, solvent A H_2O:CH_3CN:TFA = 95:5:0.1, solvent B H_2O:CH_3CN:TFA = 5:95:0.1, using a flowrate of 10 mL min^{-1} and gradient from 0–100% B over 50 min). For compounds insoluble in acetonitrile, another solvent system was used with A H_2O:CH_3OH:TFA = 95:5:0.1, solvent B H_2O:CH_3OH:TFA = 5:95:0.1, flowrate 10 mL min^{-1} using a gradient from 0–100% B over 50 min. Preparative thin layer chromatography (PTLC) was used for small amounts of products using CH_3OH:DCM = 3:97. NMR spectra were recorded using Avance DRX-500 (^{1}H: 500 MHz, ^{13}C: 125 MHz) or Avance 600 (^{1}H: 600 MHz, ^{13}C: 151 MHz) at 298 K. Chemical shifts were referenced to residual solvent peaks (CD_3OD: ^{1}H: 3.31 ppm; ^{13}C: 49.0 ppm, DMSO-d_6: ^{1}H: 2.50 ppm).

PrnF and ADH Activity

Flavin reductase PrnF from *Pseudomonas fluorescens* activity was determined in triplicates by monitoring the oxidation of NADH to NAD^+ at λ = 340 nm (ε = 6.3 mL mmol^{-1} cm^{-1}). The reactions were done in 1 mL volume containing 100 × diluted PrnF, 10 mM Na_2HPO_4 pH 7.4, 50 μM FAD and 160 μM NADH at 25 °C. Similarly, the activity of the alcohol dehydrogenase

from *Rhodococcus ruber* was based on the reduction of NAD^+ to $NADH + H^+$ at $\lambda = 340$ nm. The reaction was conducted in 1 mL volume containing 10 mM Na_2HPO_4 pH 7.4, 20% (*v/v*) isopropanol, 100 µM NAD^+ and 100 times diluted ADH. In both assays, the conversion rate of the substrate was determined by regression of the linear range 0–20 s. Reactions were conducted in triplets in a quartz cuvette with 10 mm light path.

Substrate and Halide Specificity

Reactions were done in a final volume of 200 µL containing 1 mM substrate, 30 mM NaBr, NaCl or NaI, 10 mM Na_2HPO_4 pH 7.4, 0.1 mM FAD, 0.1 mM NAD^+, 5% (v/v) isopropanol, 1000 U mL^{-1} catalase, 2.5 U mL^{-1} PrnF, 1 U mL^{-1} ADH and 8.9 mol% (5 mg mL^{-1}) *Xcc* halogenases. The reactions were incubated in a thermoshaker at 25 °C and 600 rpm for 24 h. Reactions were stopped by the addition of 200 µL methanol and the supernatant was analyzed by RP-HPLC, LC/MS or by GC/MS depending on the analyte.

Cross Linked Enzyme Aggregates Optimization (Combi-CLEAs)

The pellet from 1.5 L *E. coli* culture containing the *Xcc* halogenase with chaperones was resuspended in 30 mL of 100 mM Na_2HPO_4 (pH 7.4) and lysed three times by French Press (1000 psig). The total lysate was centrifuged (10000 × g, 30 min, 4 °C) and filtered through a 0.45 µm Whatman filter to remove cell debris. The soluble fraction was then divided into 5 fractions. 2.5 U mL^{-1} PrnF and 1 U mL^{-1} ADH were added to each fraction and mixed thoroughly. For precipitating the protein, 3.24 g (97% saturation) of ammonium sulfate was added and mixed with a tube rotator for 1 h at 4 °C. Different concentrations of glutaraldehyde (0.5, 0.8, 1, 1.25 and 1.5% (*v/v*)) were added to each fraction and mixed for additional 2 h at 4 °C. The formed Combi-CLEAs were washed 3 times with 10 mL of 100 mM Na_2HPO_4 (pH 7.4), resuspended in the same buffer and kept at 4 °C until use.

Regioselectivity Determination

Reactions were conducted in a 1 L Erlenmeyer flask at 25 °C and 150 rpm. In a final volume of 150 mL containing 0.5 mM substrate, 30 mM NaBr, 10 mM Na_2HPO_4 pH 7.4, 0.1 mM FAD, 0.1 mM NAD^+, 5% (*v/v*) isopropanol and combi-CLEAs of *Xcc* halogenase from 1.5 L culture, 2.5 U mL^{-1} flavin reductase (PrnF) and 1 U mL^{-1} (ADH) using the optimized glutaraldehyde concentration (1%). 1000 U mL^{-1} catalase was added daily. Reaction was monitored by RP-HPLC and stopped by filtration of the combi-CLEAs followed by purification of the brominated products.

Total Turnover Number (TTN) Determination

The halogenation reactions were done in triplicates in a final volume of 200 µL containing 1.7 mol% (1 mg mL^{-1}) *Xcc* halogenase, 1 mM substrate, 30 mM NaBr, 10 mM Na_2HPO_4 pH 7.4, 0.1 mM FAD, 0.1 mM NAD^+, 5% (*v/v*) isopropanol, 1000 U mL^{-1} catalase, 2.5 U mL^{-1} PrnF and 1 U mL^{-1} ADH at 25 °C for 12 h. The reactions were stopped by adding 200 µL methanol and analyzed by RP-HPLC. Product formation was calculated based on the decrease in peak area of the substrate compared to a corresponding calibration curve of each substrate.

Circular Dichroism (CD) Spectroscopy

CD spectra were recorded using a Jasco-810 CD-spectrometer with a Peltier temperature controller and a scanning speed of 100 nm min^{-1}. The measurements were performed in triplicates in a rectangular quartz cuvette with an optical path length of 1 mm at varying temperatures (25–85 °C). After IMAC purification of the halogenases, the buffer was exchanged to 10 mM Na_2HPO_4 pH 7.4 using 10 kDa cutoff Amicon Ultra centrifugal filter units to remove NaBr and imidazole and the protein concentration was adjusted to 8.9 µM (0.5 mg mL^{-1}).

Thermal Stability of the *Xcc* Halogenases

Reactions were conducted at different temperatures (25, 30, 37, and 45 °C) in a final volume of 600 µL, containing 5.7 mol% (1.6 mg mL^{-1}) *Xcc* halogenase, 0.1 mM FAD, 0.5 mM indole, 30 mM NaBr, 10 mM Na_2HPO_4 pH 7.4 and 20 mM 1-benzyl-1,4-dihydronicotinamide (BNAH) as NADH analog.[35] The reactions were stopped at distinct time intervals by addition of equal volumes of methanol, centrifuged and analyzed with RP-HPLC.

Acknowledgements

The authors thank Prof. Dr. Karl-Heinz van Pée for providing the plasmid encoding for the flavin reductase and Prof. Dr. Werner Hummel for donating the plasmid encoding for the alcohol dehydrogenase. M.I. acknowledges funding from the German Egyptian Research Long-Term Scholarship Program (GERLS) and the Bielefelder Nachwuchsfonds.

References

[1] K. Smith, G. A. El-Hiti, *Curr. Org. Synth.* **2004**, *1*, 253–274.
[2] J. M. Gnaim, R. A. Sheldon, *Tetrahedron Lett.* **1995**, *36*, 3893–3896.
[3] C. Wagner, M. El Omari, G. M. König, *J. Nat. Prod.* **2009**, *72*, 540–553.
[4] H. Sun, C. E. Keefer, D. O. Scott, *Drug Metab. Lett.* **2011**, *5*, 232–242.
[5] C. M. Harris, R. Kannan, H. Kopecka, T. M. Harris, *J. Am. Chem. Soc.* **1985**, *107*, 6652–6658.
[6] K. S. Lam, D. R. Schroeder, J. M. Veitch, J. A. Matson, S. Forenza, *J. Antibiot.* **1991**, *44*, 934–9.
[7] G. Trimurtulu, I. Ohtani, G. M. L. Patterson, R. E. Moore, T. H. Corbett, F. A. Valeriote, L. Demchik, *J. Am. Chem. Soc.* **1994**, *36*, 744–751.
[8] G. W. Gribble, in *Handb. Environ. Chem.*, Springer, Berlin, Heidelberg, **2003**, pp. 1–15.
[9] C. Schnepel, N. Sewald, *Chem. Eur. J.* **2017**, *23*, 12064–12086.

[10] T. Paneekarn, S. Chatraphorn, *Kasetsart J.* **2006**, *27*, 214–224.
[11] F. H. Vaillancourt, J. Yin, C. T. Walsh, *Proc. Mont. Acad. Sci.* **2005**, *102*, 10111–10116.
[12] M. L. Hillwig, X. Liu, *Nat. Chem. Biol.* **2014**, *10*, 921–923.
[13] M. L. Hillwig, H. A. Fuhrman, K. Ittiamornkul, T. J. Sevco, D. H. Kwak, X. Liu, *ChemBioChem* **2014**, *15*, 665–669.
[14] J. N. Carter-Franklin, A. Butler, *J. Am. Chem. Soc.* **2004**, *126*, 15060–15066.
[15] K. H. Van Pée, S. Unversucht, *Chemosphere* **2003**, *52*, 299–312.
[16] T. Dairi, T. Nakano, K. Aisaka, R. Katsumata, M. Hasegawa, *Biosci. Biotechnol. Biochem.* **1995**, *59*, 1099–1106.
[17] P. E. Hammer, D. S. Hill, S. T. Lam, K. H. Van Pée, J. M. Ligon, *Appl. Environ. Microbiol.* **1997**, *63*, 2147–2154.
[18] K. H. Van Pée, E. P. Patallo, *Appl. Microbiol. Biotechnol.* **2006**, *70*, 631–641.
[19] S. Buedenbender, S. Rachid, R. Müller, G. E. Schulz, *J. Mol. Biol.* **2009**, *385*, 520–530.
[20] P. C. Dorrestein, E. Yeh, S. Garneau-Tsodikova, N. L. Kelleher, C. T. Walsh, *Proc. Mont. Acad. Sci.* **2005**, *102*, 13843–13848.
[21] K. Podzelinska, R. Latimer, A. Bhattacharya, L. C. Vining, D. L. Zechel, Z. Jia, *J. Mol. Biol.* **2010**, *397*, 316–331.
[22] J. R. Heemstra, C. T. Walsh, *J. Am. Chem. Soc.* **2008**, *130*, 14024–14025.
[23] S. Zehner, A. Kotzsch, B. Bister, R. D. Süssmuth, C. Méndez, J. A. Salas, K. H. Van Pée, *Chem. Biol.* **2005**, *12*, 445–452.
[24] E. Yeh, S. Garneau, C. T. Walsh, *Proc. Mont. Acad. Sci.* **2005**, *102*, 3960–3965.
[25] C. Seibold, H. Schnerr, J. Rumpf, A. Kunzendorf, C. Hatscher, T. Wage, A. J. Ernyei, C. Dong, J. H. Naismith, K. H. van Pée, *Biocatal. Biotransform.* **2006**, *24*, 401–408.
[26] X. Zhu, W. De Laurentis, K. Leang, J. Herrmann, K. Ihlefeld, K. H. van Pée, J. H. Naismith, *J. Mol. Biol.* **2009**, *391*, 74–85.
[27] S. Flecks, E. P. Patallo, X. Zhu, A. J. Ernyei, G. Seifert, A. Schneider, C. Dong, J. H. Naismith, K. H. Van Pée, *Angew. Chem. Int. Ed.* **2008**, *47*, 9533–9536.
[28] S. Keller, T. Wage, K. Hohaus, M. Hölzer, E. Eichhorn, K. H. Van Pée, *Angew. Chem. Int. Ed.* **2000**, *39*, 2300–2302.
[29] C. Dong, S. Flecks, S. Unversucht, C. Haupt, K. H. van Pée, J. H. Naismith, *Science* **2005**, *309*, 2216–2219.
[30] E. Bitto, Y. Huang, C. A. Bingman, S. Singh, J. S. Thorson, G. N. Phillips, *Proteins Struct. Funct. Genet.* **2008**, *70*, 289–293.
[31] X. Chen, K. H. Van Pée, *Acta Biochim. Biophys. Sin.* **2008**, *40*, 183–193.
[32] J. Latham, E. Brandenburger, S. A. Shepherd, B. R. K. Menon, J. Micklefield, *Chem. Rev.* **2018**, *118*, 232–269.
[33] E. Yeh, L. C. Blasiak, A. Koglin, C. L. Drennan, C. T. Walsh, *Biochemistry* **2007**, *46*, 1284–1292.
[34] C. Dong, A. Kotzsch, M. Dorward, K. H. Van Pée, J. H. Naismith, *Acta Crystallogr. Sect. D* **2004**, *60*, 1438–1440.
[35] M. Ismail, L. Schroeder, M. Frese, T. Kottke, F. Hollmann, C. E. Paul, N. Sewald, *ACS Catal.* **2019**, 1389–1395.
[36] T. G. Karabencheva-Christova, J. Torras, A. J. Mulholland, A. Lodola, C. Z. Christov, *Sci. Rep.* **2017**, *7*, 17395.
[37] M. Frese, C. Schnepel, H. Minges, H. Voß, R. Feiner, N. Sewald, *ChemCatChem* **2016**, *8*, 1799–1803.
[38] P. R. Neubauer, C. Widmann, D. Wibberg, L. Schröder, M. Frese, T. Kottke, J. Kalinowski, H. H. Niemann, N. Sewald, *PLoS One* **2018**, *13*, e0196797.
[39] H. Minges, C. Schnepel, D. Böttcher, M. S. Weiß, U. T. Bornscheuer, N. Sewald, *Submitted* **2019**.
[40] M. A. Ortega, D. P. Cogan, S. Mukherjee, N. Garg, B. Li, G. N. Thibodeaux, S. I. Maffioli, S. Donadio, M. Sosio, J. Escano, L. Smith, S. K. Nair, W. A. Van Der Donk, *ACS Chem. Biol.* **2017**, *12*, 548–557.
[41] B. R. K. Menon, E. Brandenburger, H. H. Sharif, U. Klemstein, S. A. Shepherd, M. F. Greaney, J. Micklefield, *Angew. Chem. Int. Ed.* **2017**, *56*, 11841–11845.
[42] F. Leyns, M. De Cleene, J. G. Swings, J. De Ley, *Bot. Rev.* **1984**, *50*, 308–356.
[43] M. P. Starr, C. L. Jenkins, L. B. Bussey, A. G. Andrewes, *Arch. Microbiol.* **1977**, *113*, 1–9.
[44] P. A. J. Gorin, J. F. T. Spencer, B. Lindberg, F. Lindh, *Carbohydr. Res.* **1980**, *79*, 313–315.
[45] A. Becker, F. Katzen, A. Pühler, L. Ielpi, *Appl. Microbiol. Biotechnol.* **1998**, *50*, 145–152.
[46] F. J. Vorhölter, S. Schneiker, A. Goesmann, L. Krause, T. Bekel, O. Kaiser, B. Linke, T. Patschkowski, C. Rückert, J. Schmid, V. K. Sidhu, V. Sieber, A. Tauch, S. A. Watt, B. Weisshaar, A. Becker, K. Niehaus, A. Pühler, *J. Biotechnol.* **2008**, *134*, 33–45.
[47] J. T. Payne, M. C. Andorfer, J. C. Lewis, *Angew. Chem. Int. Ed.* **2013**, *52*, 5271–5274.
[48] M. Frese, P. H. Guzowska, H. Voß, N. Sewald, *ChemCatChem* **2014**, *6*, 1270–1276.
[49] L. P. Hager, D. R. Morris, F. S. Brown, H. Eberwein, *J. Biol. Chem.* **1966**, *241*, 1769–77.
[50] R. A. Sheldon, *Appl. Microbiol. Biotechnol.* **2011**, *92*, 467–477.
[51] R. A. Sheldon, *Org. Process Res. Dev.* **2011**, *15*, 213–223.
[52] M. Frese, N. Sewald, *Angew. Chem. Int. Ed.* **2015**, *54*, 298–301.
[53] R. A. Sheldon, S. van Pelt, *Chem. Soc. Rev.* **2013**, *42*, 6223–6235.
[54] J. T. Payne, M. C. Andorfer, J. C. Lewis, *Angew. Chem. Int. Ed.* **2013**, *52*, 5271–5274.
[55] T. C. Bruice, *Acc. Chem. Res.* **1980**, *13*, 256–262.
[56] D. Holtmann, F. Hollmann, *ChemBioChem* **2016**, *17*, 1391–1398.
[57] C. E. Paul, D. Tischler, A. Riedel, T. Heine, N. Itoh, F. Hollmann, *ACS Catal.* **2015**, *5*, 2961–2965.

[58] L. Tretter, V. Adam-Vizi, *Philos. Trans. R. Soc. London Ser. B* **2005**, *360*, 2335–45.
[59] L. Men, Y. Wang, *J. Proteome Res.* **2007**, *6*, 216–225.
[60] S. Dumont, N. V. Bykova, A. Khaou, Y. Besserour, M. Dorval, J. Rivoal, *PLoS One* **2018**, *13*, e0204530.
[61] D. Keilin, E. F. Hartree, *Nature* **1939**, *144*, 787–788.
[62] E. Krieger, G. Koraimann, G. Vriend, *Proteins Struct. Funct. Genet.* **2002**, *47*, 393–402.

